Phonon attenuation in amorphous solids studied by picosecond ultrasonics

C. J. Morath* and H. J. Maris
Department of Physics, Brown University, Providence, Rhode Island 02912
(Received 26 December 1995)

We have used a picosecond optical technique to measure the attenuation α of longitudinal-acoustic phonons in several disordered solids. We find a universal $\alpha \sim \nu^2$ behavior for frequencies ν up to 320 GHz and for temperatures between 80 and 300 K. Within this temperature range the phonon attenuation increases by a factor of between 2 and 3 with increasing temperature for the amorphous polymers poly(methyl methacrylate), poly(styrene), and poly(ethyl methacrylate), and for the metallic glass TiNi. We discuss our results in relation to current theories of high-frequency vibrations in glasses and thermal conduction. [S0163-1829(96)04325-1]

I. INTRODUCTION

In the 25 years since the seminal study by Zeller and Pohl,[1] much work has been devoted towards an understanding of the thermal and acoustic properties of glasses. These properties include: a specific heat $C(T)$ which varies linearly with temperature T below about 1 K; a bump in the quantity $C(T)/T^3$ around 5 K; a thermal conductivity $\kappa(T)$ varying approximately as T^2 below 1 K; and a plateau in κ between roughly 2 and 10 K followed by a rise of $\kappa(T)$ with increasing T above 10 K. The ultrasonic attenuation is much larger than in crystals, and has a complicated dependence on temperature, sound amplitude, and frequency.[2] Experiments performed on a wide variety of materials, including inorganic glasses, amorphous metals, and polymers, have established that these properties[3] are universal to disordered solids.

In the temperature range below 1 K the specific heat, thermal conductivity, and ultrasonic attenuation can all be understood[4] at a phenomenological level by the two-level-system (TLS) model introduced by Phillips[5] and by Anderson, Halperin, and Varma.[6] At higher temperatures, there is still no generally accepted explanation for the bump in $C(T)/T^3$ or for the temperature dependence of the thermal conductivity.

If it is assumed that the heat is carried by propagating modes, then the thermal conductivity can be related to the phonon attenuation $\alpha(\omega,T)$ through the kinetic formula[7]

$$\kappa(T)=\frac{1}{3}\int d\omega C(\omega,T)\Lambda(\omega,T)v, \qquad (1)$$

where $C(\omega,T)$ is the contribution to the specific heat per unit volume from phonons of angular frequency ω, $\Lambda(\omega,T)$ [equal to $\alpha^{-1}(\omega,T)$] is the mean free path of these phonons, and v is their velocity. In Eq. (1), both longitudinal and transverse phonons participate in the heat flow; since the contribution to the specific heat is greater from transverse phonons one might expect that their contribution would dominate that of the longitudinal modes. However, the possibility exists for glasses that longitudinal phonons with large Λ may provide a contribution to Eq. (1) which is significantly larger than expected from these density-of-states considerations alone. Even if one neglects differences between phonons with different polarization, from a measurement of $\kappa(T)$ it is clearly impossible to determine $\Lambda(\omega,T)$ uniquely as a function of both ω and T. If instead the relation $\kappa=\frac{1}{3}Cv\overline{\Lambda}$ is used, the average mean free path $\overline{\Lambda}$ is found to decrease rapidly[1] for temperatures in the region of the plateau. As the dominant phonon frequency $\overline{\omega}/2\pi=3k_BT/h$ approaches about 1 THz, the mean free path becomes so small that the Ioffe-Regel condition,[8] i.e., the mean free path becoming smaller than the phonon wavelength divided by 2π, is nearly satisfied. This has been taken by some authors as evidence that the propagating phonon picture becomes invalid, and alternative mechanisms of heat conduction have been proposed to describe the rise in $\kappa(T)$ above the plateau.

The soft-potential model (SPM) is a phenomenological theory capable of explaining many of the universal properties of glasses within a single framework. This theory, first proposed by Karpov, Klinger, and Ignat'ev,[9] generalizes the TLS theory by assuming a distribution of parameters which describe both single- and double-well defect states, resulting in a crossover from double-well to soft single-well potentials as the energy scale is increased. The consequences of the SPM have been investigated in several publications.[10–15] From general considerations of the distribution parameters a softmode defect density of states $g_{\rm def}(\omega)\sim\omega^4$ is calculated for frequencies just above the crossover,[11,12] leading to a specific heat that varies with temperature as T^5. In the SPM, the plateau in $\kappa(T)$ is attributed to a temperature-independent resonant scattering of phonons from the soft modes, thereby accounting in a straightforward manner for the observed correlation between the temperatures of the plateau and the bump in $C(T)/T^3$. Buchenau *et al.*[13] have shown that experimental results for $\alpha(\omega,T)$ in SiO_2 glass for a range of ω and T can be fit with the use of the same phonon-to-defect coupling constant for tunneling, relaxational, and resonant vibrational states, with no additional adjustable parameters. With the use of Eq. (1), the calculated values of $\alpha(\omega,T)$ for a-SiO_2 and a-Se were shown[13] to produce good agreement with the experimental measurements of $\kappa(T)$ at temperatures up to and including the plateau region. Karpov and Parshin[14] suggested that the rise in κ above the plateau could be caused by low-frequency ''prethermal'' phonons with large Λ, but this has been discounted[16] (at least for phonons with frequency below 0.5 THz) by measurements[17] of $\alpha(\omega,T)$ for a-SiO_2. Recently, Gil *et al.*[15]

have attributed this rise in κ to the decrease in $g_{\rm def}(\omega)/\omega^2$ observed[18] for frequencies above 3 THz.

In the formulation of the SPM discussed above, the Ioffe-Regel condition is satisfied for a narrow band of vibrational states close to the peak in $g_{\rm def}(\omega)$, whereas the highest-frequency modes are propagating. Other theories of the thermal properties of glasses predict that *all* modes above a critical frequency ω_c are localized. The fracton model of glasses, originally proposed by Alexander *et al.*,[19] postulates that glasses are self-similar[20] at length scales below a critical length $\xi \simeq v/\omega_c$. In this model, the plateau in $\kappa(T)$ is caused by a crossover at the frequency ω_c from propagating phonons to localized[21] ''fracton'' states. A bump in $C(T)/T^3$ near $T_c=\hbar\omega_c/3k_B$ has been derived in this model by various approaches.[22,23] Since the fractons are localized they can only contribute to thermal transport through anharmonic hopping processes. Perturbative calculations of the fracton hopping lifetime[24,25] predict a conductivity $\kappa_{\rm hop}(T)\sim T$, but to produce quantitative agreement with experiments for a-SiO_2 it is necessary to postulate an anharmonic coupling between phonons and fractons[25] an order of magnitude larger than the third-order elastic constants measured by ultrasonic methods.[26] Although this is troubling at first glance, experiments on the vibrations of self-similar structures[27] show that this enhanced coupling between the phonon and fracton modes could occur through a favorable overlap of their wave functions.[28] At sufficiently high temperatures (around 50 K for a-SiO_2) the lifetime broadening of the fracton states from hopping becomes so large that perturbation theory breaks down and $\kappa_{\rm hop}(T)$ increases more slowly than linearly with temperature.[25] Recently, the hopping conductivity of localized vibrational modes has been calculated beyond the perturbation limit using a model Hamiltonian system;[29] however, no quantitative comparison with experimental results was attempted.

In another approach, Allen and Feldman[30] (AF) have used the Kubo formalism to develop a theory of heat conduction in a disordered system made up of atoms connected to their neighbors by linear springs. In a numerical simulation of a-Si, Feldman *et al.*[31] found that over most of the frequency spectrum the vibrational modes were extended, but could not be sensibly assigned a velocity or wave vector for use in Eq. (1). The thermal conductivity due to these modes was calculated from $\kappa(T)=\Sigma_i C_i(T)D_i$, where $C_i(T)$ and D_i are the specific heat and the temperature-independent diffusivity of the ith mode, respectively. After D_i was calculated from the AF theory for each normal mode, the effects of TLS resonant and relaxational scattering were added into the model. The theory then gave a good description of $\kappa(T)$ as measured experimentally for a-Si from below 1 up to 150 K. In this simulation no low-frequency peak in the density of states is seen, and so the plateau in $\kappa(T)$ has to be considered to be unrelated to the bump in $C(T)/T^3$. In similar work, Sheng and Zhou[32] calculated $\kappa(T)$ using as a model a harmonic three-dimensional percolation cluster. By a suitable choice of parameters they could fit experimental results for several glasses.

Vibrational states at frequencies above 1 THz dominate the thermal transport for temperatures above the plateau in $\kappa(T)$ for all the theories we have discussed, but there are very few experiments which have studied the dynamics of these vibrations. Recently, experimental evidence for vibrational localization at frequencies above 3 THz has been found in a-Si:H at 2 K by Scholten, Akimov, and Dijkhuis[33] using time-resolved anti-Stokes Raman spectroscopy. Anharmonic lifetimes were observed to *increase* rapidly with frequency from 3 to 15 THz—a result which can be construed as evidence for localization.[33,34] If the spatial extent of the modes decreases with increasing frequency, their overlap will also decrease on average and this can lead to increased lifetimes.

Because of the lack of theoretical understanding of the universal thermal properties of glasses, it is important to have measurements of $\alpha(\omega,T)$ over as broad a range of frequencies and temperatures as possible. Such measurements can provide more detailed information than can be gained from measurements of $\kappa(T)$. Attempts have been made to use the tunnel-junction method to measure the attenuation up to 1 THz at low temperatures, typically below 2 K. However, various tunnel-junction studies of a-SiO_2 have led to widely different results for the frequency dependence of the attenuation and disagree as to whether the scattering of phonons is predominately elastic[35,36] or inelastic.[37,38] At higher temperatures, measurements have been performed up to around 30 GHz by Brillouin scattering.[39] The attenuation in a-SiO_2 at higher frequencies and for temperatures above 80 K was studied using picosecond optical techniques by Zhu, Maris, and Tauc.[17] They found a quadratic dependence of the attenuation on frequency from 76 to 440 GHz with no significant temperature dependence from 80 to 300 K. In this paper we report on similar measurements for other amorphous materials in order to investigate the possible universality of this high-temperature attenuation. The samples are three amorphous polymers and a metallic glass, and the attenuation is measured for frequencies up to 320 GHz in the temperature range from 80 to 300 K. For all the samples studied we find a quadratic frequency dependence of the attenuation. For the polymers the magnitude of this attenuation is found to be much larger than for a-SiO_2,[17] and mean free paths as short as 70 Å are observed.

II. EXPERIMENT

A. Apparatus

The experimental setup for measurements on transparent samples is shown schematically in Fig. 1. The samples are thin films of amorphous polymers deposited onto substrates. A thin Al film is evaporated on the sample surface for use as a transducer. A longitudinal-acoustic wave is launched into the sample when a subpicosecond ''pump'' light pulse is focused onto a small area of the transducer film, causing it to rapidly heat and expand. The strain propagates into the sample and a fraction $r_{\rm FS}$ is reflected at the interface between the sample film and substrate. On returning to the transducer the strain causes a small change in the optical reflectivity. This change is detected by means of a ''probe'' light pulse which is time delayed relative to the pump pulse. By varying the time delay t of the probe a measurement of the time-dependent reflectivity $\Delta R(t)$ is obtained for the sample. The magnitude of $\Delta R/R$ is on the order of 10^{-5} so that it is necessary to use modulation techniques together with signal

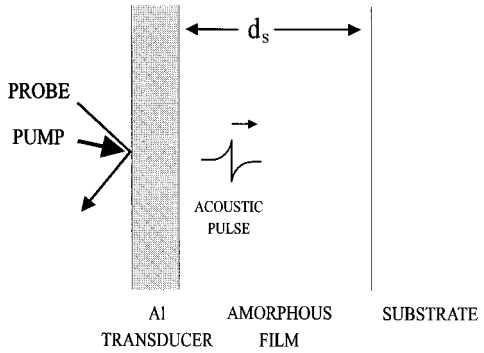

FIG. 1. Schematic diagram of the experiment for transparent sample films.

averaging to obtain accurate measurements. Typical data $\Delta R(t)$ are shown in Fig. 2 for a 620 Å film of poly(methyl methacrylate) on a Al_2O_3 substrate with a 170 Å Al transducer. For the opaque TiNi samples the pump pulse can be absorbed directly at the sample surface and no transducer film was used.

As a stable source of light pulses we use a Ti:sapphire mode-locked laser,[40] operating at approximately 750 nm with a repetition rate of 76 MHz. The light pulses have an autocorrelation width of 200 fsec, with typical pulse energies of 0.5 nJ for the pump and 0.1 nJ for the probe. The pump and probe pulses are focused to a spot of diameter 20 μm on the sample surface. Given these experimental conditions it is straightforward to show[17] that the steady-state heating of the samples is small (less than 5 K) at ambient temperatures above 80 K. At lower temperatures the effects of laser heating become progressively more important because of the rapidly decreasing heat capacity of the sample and the increasing thermal boundary resistance between sample and substrate.

B. Sample preparation and characterization

The polymer samples, either poly(methyl methacrylate) (PMMA),[41] poly(styrene) (PS),[42] or poly(ethyl methacrylate) (PEMA),[43] were spin-coated from solution onto either Al_2O_3, Si, or GaAs substrates. Chlorobenzene was used as solvent for the PMMA, whereas methyl ethyl ketone was used for the PS and PEMA solutions. The solutions contained between 0.5 and 4% polymer by volume; the polymer concentration was chosen to obtain the desired sample thickness (from 295 to 1470 Å). The coated substrates were spun at 4500 rpm for 30 s and then baked to remove the solvent and to improve the film uniformity. The samples were baked for 2 h at temperatures of 120 °C for PMMA, and 110 °C for films of PS and PEMA. The film thicknesses d_s for samples on Si and GaAs were measured by ellipsometry. The thickness was found to be uniform over a 1 cm^2 area to within $\pm 5\%$. Atomic-force microscopy measurements with lateral scale 10 μm yielded approximate rms surface roughnesses of 5 and 10 Å for PMMA films of thickness 350 and 620 Å, respectively. In the next section we will return to discuss the effects of surface and interfacial roughness on the attenuation measurements.

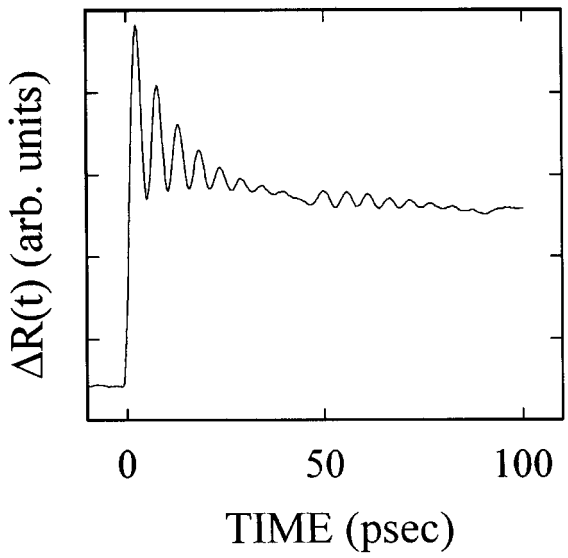

FIG. 2. Change in reflectivity versus time $\Delta R(t)$ for a 180 Å Al transducer on a 620 Å PMMA film on a Al_2O_3 substrate.

TABLE I. Summary of sample properties and frequencies of measurement. For the TiNi samples the measurement frequencies are taken from the Fourier transforms of the acoustic echoes as described in the text.

Sample	Substrate	d_s (Å)	Frequency (GHz)
PMMA	Al_2O_3	1 450	89, 92, 114
PMMA	Al_2O_3	620	136, 188
PMMA	Al_2O_3	350	232, 265, 320
PS	GaAs	1 345	80
PS	GaAs	690	132
PS	GaAs	305	109, 116, 150, 174, 189
PEMA	GaAs	690	94, 123, 154
PEMA	Si	680	80, 104, 113, 119
PEMA	Si	295	175, 213, 255
TiNi	Si	28 900	33, 50
TiNi	Si	12 900	83, 99
TiNi	Si	2 300	175, 200

Films of the amorphous[44] metallic alloy TiNi were sputtered[45] onto prime grade (100) Si substrates. Stylus profilometry was used to measure the sample thickness d_s and this was found to be uniform to within $\pm 10\%$ over the 2 inch wafers.

The Al transducer films, with thicknesses d_{Al} ranging from 100 to 400 Å, were resistively evaporated onto the polymer samples in a vacuum of better than 5×10^{-6} Torr at growth rates of 3 to 10 Å s^{-1}. The thinner transducers were used to study the attenuation of higher frequency acoustic waves. The samples which were used to study the attenuation are listed in Table I along with the respective frequencies of measurement.

C. Data analysis

The data $\Delta R(t)$ shown in Fig. 2 have an oscillatory acoustic component with a frequency given by $\omega_0/2\pi = v_{Al}/2d_{Al}$, where v_{Al} is the longitudinal sound velocity in Al. There exists a large acoustic mismatch between Al and PMMA so that only a small fraction of the strain is transmitted into the PMMA during each Al vibrational pe-

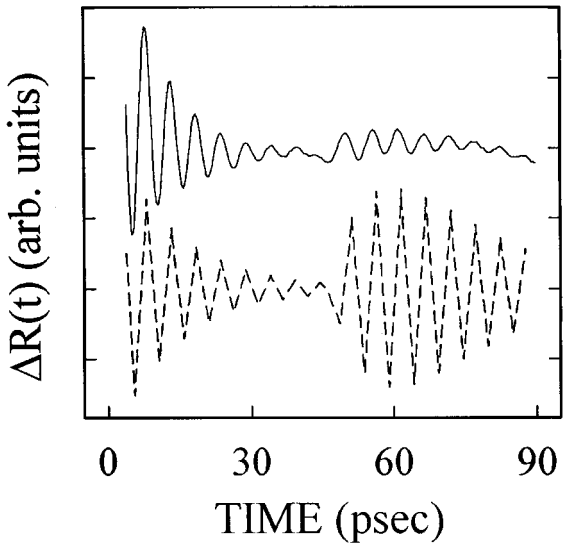

FIG. 3. Solid line: acoustic contribution to $\Delta R(t)$ for the data shown in Fig. 2. Dashed line: result from the numerical simulation used in Eq. (2) to calculate the attenuation.

riod. As a result the Al vibrations are slowly damped and this allows the quantity ω_0 to be precisely defined. To vary the measurement frequency $\omega_0/2\pi$ for a given sample, Al is evaporated in different thicknesses on separate areas of the polymer surface.

For a given polymer sample and transducer, the following procedure is used to determine the attenuation $\alpha(\omega_0)$ from the data $\Delta R(t)$. As a first step in the data analysis, the slowly varying background in Fig. 2 is fit to a polynomial and then subtracted from the raw data, leaving only the acoustic contribution. The background arises because there is a contribution to ΔR from the change in temperature of the Al film. This temperature slowly relaxes as the heat flows from the Al through the polymer and into the substrate. The result of this subtraction procedure applied to the data of Fig. 2 is given by the solid line in Fig. 3.

We then compare these acoustic data to results obtained from a numerical simulation in which it is assumed that there is no attenuation in the sample film. The simulation time develops the one-dimensional equations of elasticity for the structure, taking the initial strain distribution to be constant in the transducer film and zero elsewhere. The change in reflectivity is taken to be proportional to the total strain in the transducer film. The inputs to the simulation are the thicknesses d_s and d_{Al}, along with the densities ρ and longitudinal sound velocities v for the transducer, sample, and substrate. Room-temperature values of ρ and v for the materials we have used are listed in Table II. We use bulk values of ρ for the polymers, and of ρ and v for the substrates and Al transducer. Values of v_s and d_s listed in Table II for the polymer samples are determined experimentally as discussed below. Results of the simulation are shown by the dashed line in Fig. 3 for a 180 Å Al transducer on a 620 Å PMMA film on a Al_2O_3 substrate.

To determine the attenuation our approach is to compare the ratio of the amplitude $A^{(0)}$ of the initial ringing of the transducer to the amplitude $A^{(1)}$ of the first acoustic echo as calculated in the simulation with the same ratio measured

TABLE II. Density ρ and room-temperature longitudinal sound velocity v used in calculation of the attenuation. For the polymers and for a-TiNi, v was determined from our measurements as discussed in the text.

Material	ρ (g cm^{-3})	$v(10^5$ cm s$^{-1})$
Al	2.7	6.4
Si (100)	2.33	8.43
GaAs (100)	5.31	4.73
Al_2O_3 (1000)	3.98	11.2
a-TiNi	6.3	5.54 ± 0.03
PMMA	1.18	2.83 ± 0.08
PS	1.1	2.41 ± 0.09
PEMA	1.05	2.62 ± 0.10

experimentally. The attenuation rate $\alpha(\omega_0)$ of the energy of the sound wave per unit distance is then

$$\alpha(\omega_0)=\frac{1}{d_s}\ln\left[\frac{A^{(1)}_{\mathrm{sim}}/A^{(0)}_{\mathrm{sim}}}{A^{(1)}_{\mathrm{exp}}/A^{(0)}_{\mathrm{exp}}}\right]. \tag{2}$$

One difficulty in this approach arises from the long ringing time of the transducer. For the thin polymer samples the ringing of the transducer has not completely damped out at the time that the first acoustic echo appears. To correct for this, the initial transducer oscillations are fit to a cosine function multiplied by a decaying exponential. This fit is then subtracted from the experimental data in the time range where the first acoustic echo appears so that a better estimate of the true amplitude of the acoustic echo can be obtained.

The longitudinal sound velocity v_s for each sample was determined from the relation

$$d_s=\frac{v_s\tau}{2}, \tag{3}$$

where τ is the round-trip acoustic transit time through the sample and is calculated from $\Delta R(t)$. For each polymer sample the velocity v_s was first calculated from Eq. (3) using the value d_s measured by ellipsometry. It was found that v_s determined in this manner for samples with $d_s<400$ Å was consistently 10 to 20% higher than v_s found for samples with $d_s>600$ Å . These variations could be caused by real structural differences between thin and thick polymer films, for example from strain near the polymer/substrate interface. However, it is well known that ellipsometry becomes increasingly sensitive to error as the film thickness is decreased[46] and we assumed that this was the source of the discrepancies observed for v_s. To calculate d_s for use in the simulation and in Eq. (2), we thus used Eq. (3) with v_s determined for each polymer from an average of measurements on samples thicker than 600 Å . These average values of v_s for the polymers are listed in Table II. The experimental uncertainties for v_s determined in this manner are less than 5% for all three polymers. If instead the ellipsometry values for d_s are correct, then our results for $\alpha(\omega)$ are 10 to 20% too large for the samples with $d_s<400$ Å as given in Table I.

For the TiNi samples we use a different procedure to analyze the data. In Fig. 4 the measured $\Delta R(t)$ is shown for a

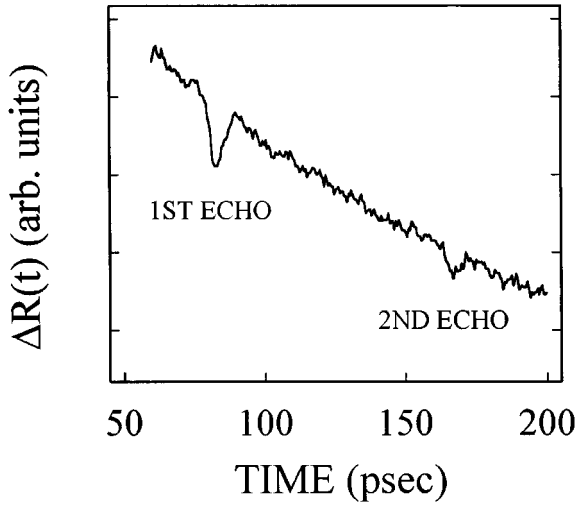

FIG. 4. Change in reflectivity versus time $\Delta R(t)$ for a 2300 Å a-TiNi film on a Si substrate. A wavelength of 750 nm was used for both the pump and probe.

2300 Å a-TiNi film on Si. The data were taken with a wavelength of 750 nm for both the pump and probe. To determine the attenuation we subtract the slowly varying thermal background and calculate the Fourier transforms ΔR_1 and ΔR_2 of the first and second acoustic echoes, respectively. The attenuation is given by[17,47]

$$\alpha(\omega)=\frac{1}{d_s}\ln\left[\frac{r_{\mathrm{FS}}\Delta R_1(\omega)}{\Delta R_2(\omega)}\right]. \tag{4}$$

The stylus profilometry values for d_s are used in Eq. (3) to calculate the value $v_s=5.54(\pm 0.03)\times 10^5$ cm/s included in Table II. To calculate r_{FS} we use acoustic mismatch theory with the densities and longitudinal sound velocities for TiNi and Si listed in Table II.

Acoustic waves with Fourier components in a range from approximately 30 to 90 GHz can be generated and detected in the TiNi samples when a laser wavelength around 750 nm is used. For a given material this range is determined by a combination of the elastic properties and the optical constants at the pump and probe wavelengths.[47] Measurements with 750 nm light were made on TiNi samples of thicknesses 28 900 and 12 900 Å as listed in Table I. To make measurements at higher frequencies, the pump and probe laser pulses were frequency doubled to a wavelength of 400 nm. For the TiNi sample of thickness 2300 Å this wavelength was used to measure $\alpha(\omega)$ at frequencies of 175 and 200 GHz.

III. RESULTS

A. Acoustic attenuation

Results for the attenuation as a function of frequency at 300 K are shown in Fig. 5 for PMMA, PS, PEMA, and a-TiNi. We have also included the results for a-SiO_2 from Zhu, Maris, and Tauc.[17] For clarity the PS results have been offset as indicated in Fig. 5. The procedure used to calculate the error bars will be described later below. We find a quadratic dependence of the attenuation on frequency for all the

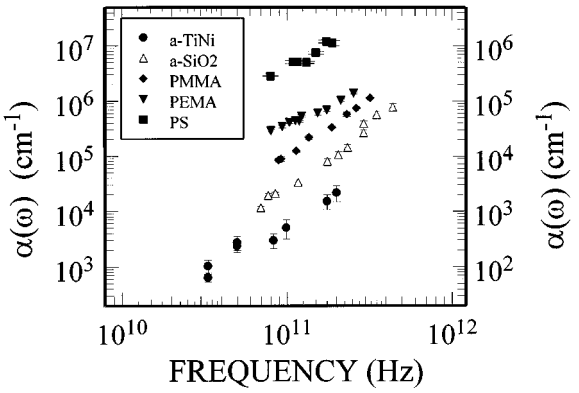

FIG. 5. Phonon attenuation as a function of frequency at 300 K for PMMA, PS, PEMA, and a-TiNi. Also shown are the results for a-SiO_2 (Ref. 17). The results for PS have been offset for clarity, and are plotted in accordance with the scale on the right.

glasses we have studied. The only significant deviation from the quadratic behavior is observed for PEMA at frequencies below 150 GHz.

The variation of the attenuation with temperature is shown in Figs. 6, 7, and 8 for PMMA, PS, and PEMA, respectively. For PMMA the attenuation increases by approximately a factor of 2 with increasing temperature from 80 to 300 K, for the frequencies 89, 136, 188, and 232 GHz. For PS and PEMA, similar variations of α within the same temperature range can be seen in Fig. 7 for frequencies of 116 and 189 GHz, and in Fig. 8 for a frequency of 154 GHz. For the metallic glass TiNi we have found that α increases by approximately a factor of 3 with increasing temperature from 80 to 300 K for frequencies near 200 GHz. We have not attempted to measure the temperature dependence of the attenuation in TiNi at lower frequencies because α is already very small at 300 K and is close to the limit of detection in our experiments.

Figures 6 and 7 show that the temperature variations of α for PMMA and PS are independent of frequency to within

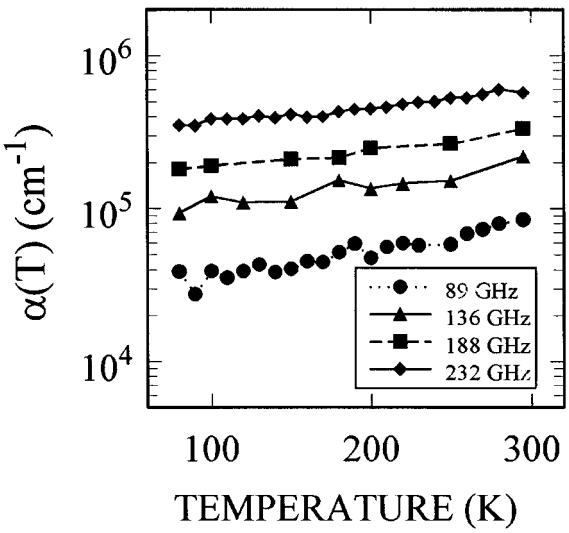

FIG. 6. Phonon attenuation in PMMA as a function of temperature. The data at frequencies of 89, 136, 188, and 232 GHz are from samples as listed in Table I.

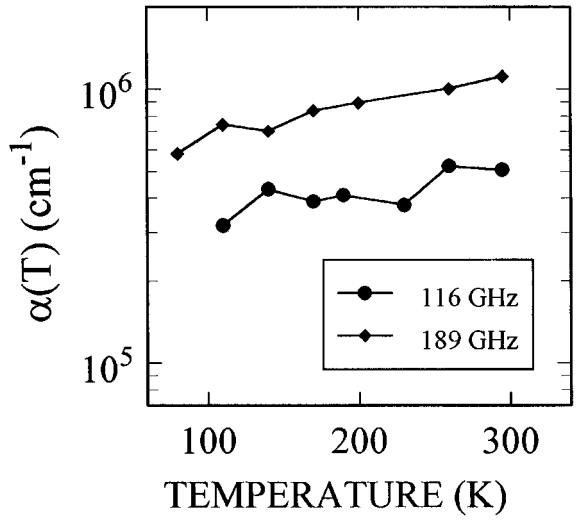

FIG. 7. Phonon attenuation in PS as a function of temperature. The data at frequencies of 116 GHz and 189 GHz are from samples as listed in Table I.

the experimental error. Thus the quadratic frequency dependence of α is found to hold for these polymers within the entire temperature range from 80 to 300 K. As is shown in Fig. 5, an attenuation varying roughly quadratically with frequency was found in the earlier measurements[17] for a-SiO_2, for frequencies from 76 to 440 GHz and temperatures between 80 and 300 K. No significant variation of α with temperature within this temperature range was observed for a-SiO_2.

To check for a dependence of the attenuation on acoustic intensity, measurements were performed on PMMA at 300 K for pump pulse energies from 0.4 to 1.3 nJ. No variation of α was observed within this range of pump intensities, which corresponded to strains from 1 to 3 $\times 10^{-4}$ and acoustic intensities from 5 to 15 $\times 10^{-6}$ W/cm^2. Since our time-resolved technique is phase sensitive, both elastic and inelastic processes can contribute to the α we have measured, and cannot be distinguished *a priori* in the data.

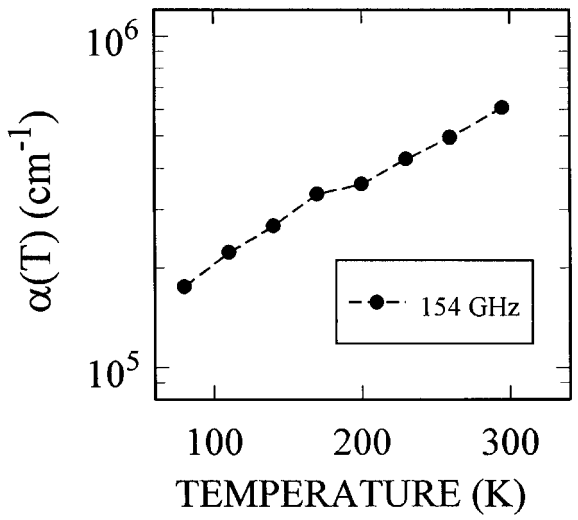

FIG. 8. Phonon attenuation in PEMA at 154 GHz as a function of temperature.

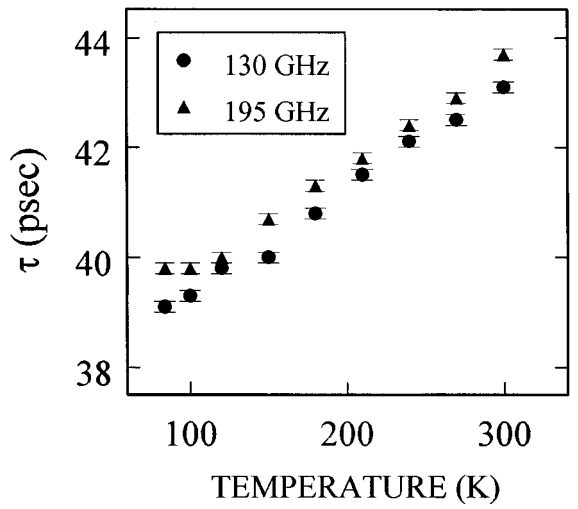

FIG. 9. Round-trip acoustic transit time $\tau(T)$ versus temperature for a sample of PMMA with thickness $d_s \approx 600$ Å on a Al_2O_3 substrate for frequencies of 130 and 195 GHz.

B. Temperature and frequency dependence of the sound velocity for polymers

We have measured the temperature dependence of the sound velocity in PMMA for the frequencies 130 and 195 GHz. To do this, two Al transducers with different thicknesses (yielding different frequencies of measurement) are evaporated on a sample of PMMA. The transducers are deposited in close proximity (within 0.5 cm) to minimize the difference in the underlying sample thickness. In Fig. 9 we have plotted the measured acoustic round-trip time for a PMMA film approximately 600 Å thick, for temperatures between 80 and 300 K. It can be seen that the curves for the transit time $\tau(T)$ at the two frequencies have an approximately constant separation of less than 0.2 ps, independent of temperature. To within experimental error the difference in the acoustic transit time is consistent with the thickness gradient of the sample as measured by ellipsometry. Thus, there is no evidence for velocity dispersion within this range of frequencies and temperatures.

The temperature dependence of the velocity is most conveniently discussed in terms of the temperature derivative $\beta(T)$ of the logarithm of the sound velocity. The data for PMMA in Fig. 9 give the result

$$\beta(T) \equiv \frac{1}{v_s}\frac{dv_s}{dT} = -5\times 10^{-4}\ \mathrm{K}^{-1} \tag{5}$$

over the temperature range 80 to 300 K. In the determination of this value no correction was made for the dependence of sample thickness on temperature. The bulk coefficient of thermal expansion for PMMA (Ref. 48) is approximately 5×10^{-5} K^{-1} within the temperature range investigated, so that the variation in d_s with temperature can be safely neglected. The above value of $\beta(T)$ is in good agreement with the value found for PMMA at Brillouin frequencies.[49] Higher precision experiments[50] at MHz frequencies find a similar value of $\beta(T)$ for temperatures down to 120 K. Below this temperature there is a rather sudden drop in β to a value of -2.8×10^{-5} K^{-1}, and β remains almost constant at

this value down to 4 K.[50] Another abrupt change in the value of $\beta(T)$ is observed[51] for PMMA at the glass transition temperature, $T_g \simeq 380$ K. We will return in Sec. IV B to discuss the temperature dependence of the sound velocity in glasses in relation to the fracton model. A similar analysis for PS and PEMA in the temperature range from 80 to 300 K gives approximately constant values for $\beta(T)$ of -7×10^{-4} K^{-1} and -9×10^{-4} K^{-1}, respectively.

C. Error analysis

A discussion of some possible sources of error in this type of experiment has been given previously in Ref. 17. The most difficult errors to eliminate can arise from the acoustic quality of the interfaces in the structure. To calculate the attenuation from the data, we have used the acoustic-mismatch value for r_{FS}. If there is acoustic loss at the interfaces or poor contact between layers, the true value of r_{FS} will differ from this value and our result for the attenuation will be in error. These errors will be minimized when the attenuation experienced by the acoustic wave in the bulk sample is very large. This favors the use of a very thick sample, such that $\alpha d_s \gg 1$. An upper limit for αd_s occurs when the amplitude of the returning echo becomes comparable to the noise in the experiment.

It is found that the results for α on polymer samples thin enough to satisfy the condition $\alpha d_s < 1$ are usually higher than for samples with $\alpha d_s > 1$. These differences in the measured attenuation are consistent with a value of r_{FS} approximately 10% below the acoustic-mismatch value, and hence are consistent with some acoustic loss at the interfaces. To minimize the measurement errors as discussed above, we use polymer samples for which the condition $2 < \alpha d_s < 4$ is satisfied. The estimated error bars shown in Fig. 5 have been calculated for each data point by varying r_{FS} by $\pm 10\%$ from the acoustic-mismatch value.

In principle, the *roughness* of the interfaces provides a source of error which is very difficult to eliminate. Acoustic loss occurs in a rough sample since various parts of the acoustic wave travel different path lengths through the sample and become out of phase. Since the variations in path length due to roughness can vary with sample thickness, this error cannot be easily eliminated, even by measurements on a set of samples with varying d_s. In our experiments we have used very smooth substrates of Al_2O_3, Si, and GaAs to minimize the scattering of the acoustic wave at the sample to substrate interface. The Al_2O_3 substrates[52] had rms roughnesses[53] of 4 to 6 Å over a lateral scale of 50 μm. The Si substrates were prime grade (semiconductor industry standard) with rms surface roughnesses estimated to be below 5 Å, based on a study of similar wafers.[54] The roughnesses of the GaAs substrates are believed to be in a similar range. In any event, measurements on samples with GaAs as the substrate gave attenuation results consistent with the values found on similar samples with Al_2O_3 or Si as the substrate.

To investigate the effect of roughness at the sample to transducer interface we have studied a series of amorphous polymer samples with various surface roughnesses σ and correlation lengths ζ of the roughness. These samples were vapor deposited on Si substrates and characterized using atomic force microscopy (AFM) by Collins *et al.*[55] At a frequency of 70 GHz (d_{Al} = 470 Å), we found consistent attenuation results from measurements on two samples which had values (d_s, σ, ζ) respectively of (7500, 51, and 90 Å) and (7900, 16, and 40 Å). For both these samples the condition $\alpha d_s \simeq 4$ was satisfied at 70 GHz. The polymer samples used for our measurements have comparable values of the product αd_s and similar, or smaller, values of σ/d_{Al} and σ/d_s. This gives us confidence that surface roughness does not contribute significantly to the results for α shown in Fig. 5. In addition, the observed dependence of α on temperature for the samples appears to rule out the possibility that the attenuation is dominated by interfacial scattering, or by any other scattering process not intrinsic to the amorphous sample.

IV. DISCUSSION

A. Comparison with other data

We first compare our results with other data to try to get an overview of the dependence of the phonon attenuation $\alpha(\omega,T)$ on frequency and temperature. Several groups have performed experiments to study phonon propagation in glasses using tunnel-junction (TJ) techniques. These measurements can be made in a frequency range which overlaps ours, but the temperature range is usually limited to below 2 K. Many of the TJ attenuation measurements[35–38] have been performed for transverse phonons in a-SiO_2, and have found widely differing frequency dependences of the attenuation (from $\omega^{2.9}$ to ω^6). These experiments also disagree as to whether the phonon scattering is elastic or inelastic. Nevertheless, for a-SiO_2 the attenuation as measured by all these TJ experiments is significantly smaller than the attenuation as measured in the same frequency range at higher temperatures by Zhu, Maris, and Tauc.[17]

Results of a number of measurements on PMMA are shown in Fig. 10. Tunnel junction experiments at a temperature of around 1 K have been performed for PMMA by Scherg *et al.*,[56] who used a stress-tuned spectrometer to distinguish between longitudinal and transverse phonons. The attenuation was observed to vary as $\omega^{4.5}$ for transverse phonons and as ω^6 for longitudinal phonons. Also included in the figure are Brillouin-scattering results for longitudinal phonons[57,58] at 1 and at 300 K, along with the estimate of the attenuation obtained[59] from the thermal conductivity of PMMA. The TC results for the attenuation at frequency ω have an effective temperature of $T = \hbar\omega/3k_B$, i.e., roughly 2 to 8 K for the frequency range from 100 to 500 GHz. It can be seen that the TJ results for the attenuation of transverse phonons are in close agreement with the thermal conductivity fit, although considering the status of the TJ measurements for a-SiO_2 no definitive conclusions can be drawn from this agreement. However, in Fig. 10 the attenuation of longitudinal phonons does, in general, appear to be substantially smaller than the attenuation of transverse phonons.

The results in Fig. 10 also show a significant increase in the attenuation of longitudinal phonons with increasing temperature from 1 to 300 K. In our measurements for PMMA we find an increase of only a factor of 2 for the attenuation as the temperature is increased from 80 to 300 K. The attenuation we measure at 80 K is typically an order of magnitude

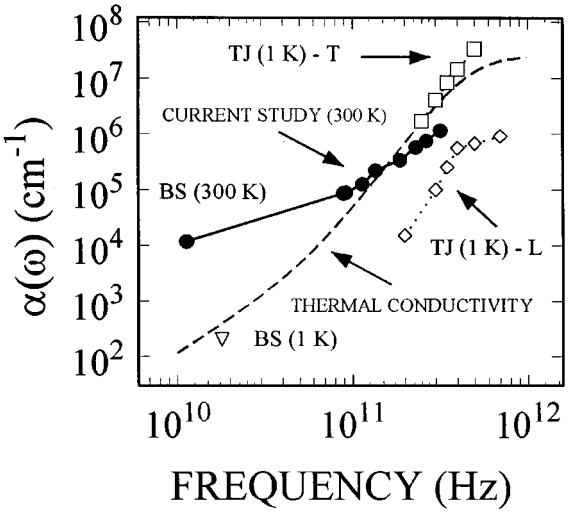

FIG. 10. Attenuation results for PMMA from a number of different techniques. The dashed line is the estimate of the attenuation from a fit to the thermal conductivity of PMMA (Ref. 59). The measurements of the present paper and the Brillouin-scattering (BS) measurements (Ref. 58) are taken at a temperature of 300 K and are denoted by ●. The Brillouin-scattering measurements at 1 K (Ref. 57) are denoted by ▽. The tunnel-junction (TJ) measurements at 1 K (Ref. 56) are denoted by □ for transverse (T) and by ◇ for longitudinal (L) phonons.

larger than the attenuation measured by the TJ experiment at 1 K. Thus a more rapid variation of the attenuation with temperature is required in the range between 1 and 80 K than in the range between 80 and 300 K. We next turn to discuss the frequency dependence of this high-temperature attenuation.

In Fig. 11 we show the attenuation in PMMA, PS, PEMA, and TiNi over a broad frequency range, for a temperature of 300 K. We have also included the frequency dependence of the attenuation at 90 K for a-SiO_2.[17] The results below 20 GHz are from ultrasonic[51] and Brillouin-scattering[60] experiments. The results for α from the various techniques form a consistent pattern for all the glasses. At low frequencies α has a dependence on frequency which is close to linear, changing above 10 to 50 GHz to the quadratic frequency dependence we observe. For frequencies below approximately 1 GHz, the attenuation results have been interpreted in terms of different models of relaxing structural defects.[61] However, difficulties arise when attempting to interpret the Brillouin-scattering results using such a theory.[62,63] Further problems of attempting to explain the attenuation above 80 GHz in a-SiO_2 with a relaxation theory have been previously discussed.[17] In the case of PMMA, to account for the quadratic frequency dependence of the attenuation as observed up to 320 GHz, most of the defects would need to have relaxation times satisfying the condition $\tau_{\rm rel} \ll 5\times10^{-13}$ s. Since a typical attempt frequency is in the THz range, it is very unlikely that the experimental results for α can be explained by any theory of relaxing defects.

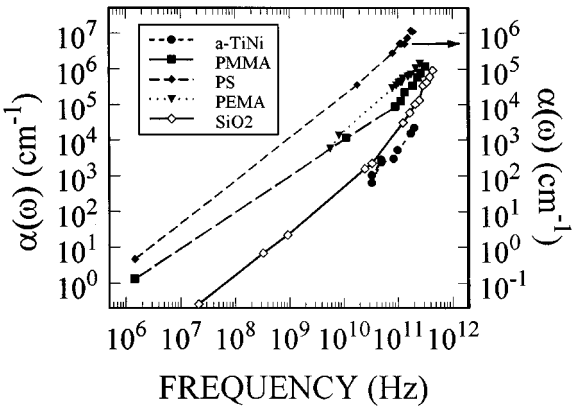

FIG. 11. Attenuation versus frequency in PMMA, PS, PEMA, and a-TiNi over a broad frequency range for a temperature of 300 K. Also shown are results for a-SiO_2 at 90 K (Ref. 17). Low-frequency results are from Brillouin-scattering measurements (Ref. 60) and ultrasonic measurements (Ref. 51). The quantity plotted is the rate of attenuation of the energy of the sound wave with distance.

B. Comparison of results with the fracton model

Attempts have been made to explain the strong attenuation found in glasses for Brillouin frequencies and high temperatures in terms of anharmonic processes. For many crystals, the attenuation results can be adequately explained by processes which couple three acoustic phonons;[64] however, to account for the Brillouin-scattering (BS) results for a-SiO_2 in this manner requires[62] an unreasonably large value of the Gruneisen parameter ($\gamma \simeq 200$). For Perovskite crystals a strong attenuation is observed[65] which is difficult to explain by three phonon processes involving acoustic phonons. Barrett[65] has attributed the attenuation to an anharmonic coupling between acoustic phonons and the soft optic modes which are found in such crystals. It has been proposed[66] that the BS results for a-SiO_2 can be explained in a similar way by anharmonic coupling of the acoustic phonons with optic modes. This theory requires a very short lifetime for the optic modes (10^{-13} s), but it is uncertain whether this condition is satisfied for glasses.

Anharmonic scattering processes have also been considered within the fracton model of glasses.[24,25] This microscopic model[19] postulates that glasses are self-similar, either in the mass density or in the connectivity between atoms, at length scales shorter than a crossover length ξ. In analogy with percolation networks, at length scales larger than ξ the glass looks homogeneous and the vibrational modes are propagating phonons. For length scales smaller than ξ the vibrational modes are localized[21] excitations on the fractal geometry. A frequency $\omega_c = 2\pi v/\xi$ is associated with the crossover from phonons with $\omega < \omega_c$ to fractons with $\omega > \omega_c$, where v is the phonon velocity. Using perturbation theory, Jagannathan *et al.*[25] have found that at temperatures high enough that $k_B T/\hbar\omega_c > 1$, the attenuation of phonons is dominated by the process

$$\text{phonon} + \text{fracton} \rightarrow \text{fracton}' . \tag{6}$$

In this temperature range the fractons make a hopping contribution to the thermal conductivity $\kappa_{\rm hop}(T)$ which is proportional to T, and the phonon attenuation is given by the expression

$$\alpha_{\rm fr}(\omega,T)=\frac{2\pi}{\omega_c^3 k_B}P(\bar{\bar{d}},D,d_\phi)\omega^2\kappa_{\rm hop}(T). \qquad (7)$$

The coefficient $P(\bar{\bar{d}},D,d_\phi)$ is a function of the fracton (spectral) dimension $\bar{\bar{d}}$, the fractal dimension D, and the superlocalization exponent d_ϕ, and is found[25] to have the value $P=0.09$ when $\bar{\bar{d}},D$, and d_ϕ are given values for a three-dimensional percolating network (4/3, 2, and 1.75, respectively). The value of P depends only weakly on these parameters. The other quantities in Eq. (7) can be calculated from experimental measurements as described later; thus the predictions of the fracton model can be compared with our results for $\alpha(\omega,T)$ using essentially no free parameters. In particular, the anharmonic coupling coefficient, which enters into the fracton model as an adjustable parameter in the constant of proportionality between $\kappa_{\rm hop}(T)$ and T, does not enter into Eq. (7).

The perturbative approach leading to Eq. (7) is valid for temperatures above the plateau in $\kappa(T)$, provided that $\omega_c\tau_{\rm fr}(T)>1$, where $\tau_{\rm fr}$ is the fracton hopping lifetime.[25] As the temperature is increased, $\tau_{\rm fr}$ decreases and perturbation theory begins to break down at a temperature T_0. For temperatures slightly above T_0 [i.e., to first order in $(\omega_c\tau_{\rm fr})^{-1}$], Jagannathan *et al.*[25] find that Eq. (7) should still hold, but the hopping conductivity should increase more slowly than linearly with temperature, i.e., a ''rollover'' of $\kappa_{\rm hop}(T)$ should occur at T_0. Such a temperature dependence for the thermal conductivity is observed for many glasses. Furthermore, Freeman and Anderson[67] (FA) have found that the experimental values of $\kappa(T)$ for many amorphous solids can be scaled to a single universal curve for temperatures above the plateau by plotting $\kappa(T)v/\Theta_D^2$ as a function of the quantity T/Θ_D, where Θ_D is the Debye temperature. For many different glasses the rollover of $\kappa(T)$, and hence the breakdown of perturbation theory, is found to occur when a temperature of $T_0\simeq 0.15\Theta_D$ is reached. For a-SiO_2 this temperature is approximately 50 K.

If the rise in thermal conductivity above the plateau is due to the phonon-assisted hopping of localized modes, then it may also be expected that our results for α would scale with T/Θ_D. For this reason, in Fig. 12 we have compared our attenuation results to the fracton predictions together for the various glasses as a function of T/Θ_D. We have plotted for PMMA, PS, TiNi, and a-SiO_2 the ratio $\alpha/\alpha_{\rm fr}$, i.e., the ratio of the observed magnitude of the ω^2 attenuation to the magnitude of the ω^2 attenuation as predicted from Eq. (7). For PMMA, PS, and a-SiO_2, we have used values of θ_D as given by Freeman and Anderson.[67] For TiNi we calculate Θ_D from the measured value of v_s assuming the velocity for transverse phonons to be given by $v_t=\frac{1}{2}v_s$. The values of T/Θ_D in Fig. 12 range from approximately 0.2 for a-SiO_2 for a temperature of 80 K, to 5 for PMMA and PS for a temperature of 300 K. To calculate $\alpha_{\rm fr}$ from Eq. (7) we assume $P=0.09$ and determine $\kappa_{\rm hop}(T)$ and ω_c for each glass as follows. The conductivity $\kappa_{\rm hop}(T)$ due to the hopping of fractons is taken to be the experimental value of $\kappa(T)$ minus the contribution due to phonons. We estimate the phonon contribution to be the value of the conductivity $\kappa_{\rm plateau}$ at the plateau. This simple procedure neglects the increase in attenuation of the phonons with temperature, but should only slightly underestimate $\kappa_{\rm hop}(T)$. For PMMA and a-SiO_2, we have used values of $\kappa(T)$ and $\kappa_{\rm plateau}$ as measured by Cahill and Pohl[68] to calculate $\kappa_{\rm hop}(T)$. Accurate measurements[69] of $\kappa(T)$ for PS are only available below 100 K, so in this case the FA scaling relation has been used to extrapolate $\kappa(T)$ into the temperature range from 100 to 300 K. For TiNi, experimental results are not available for the nonelectronic contribution to $\kappa(T)$, so we have taken the nonelectronic thermal conductivity values[70] for another metallic glass (PdSi) and applied the FA scaling procedure to estimate $\kappa(T)$. To calculate ω_c for use in Eq. (7) for PMMA, PS, and a-SiO_2 we have used the experimental values for v_s along with the values for ξ as obtained by Graebner *et al.*[59] from fits to the thermal conductivity. For TiNi, we have used the values of $\kappa(T)$ as estimated above, along with a fitting procedure similar to the one used by Graebner *et al.* to obtain the value $\xi = 20$ Å for the calculation of ω_c.

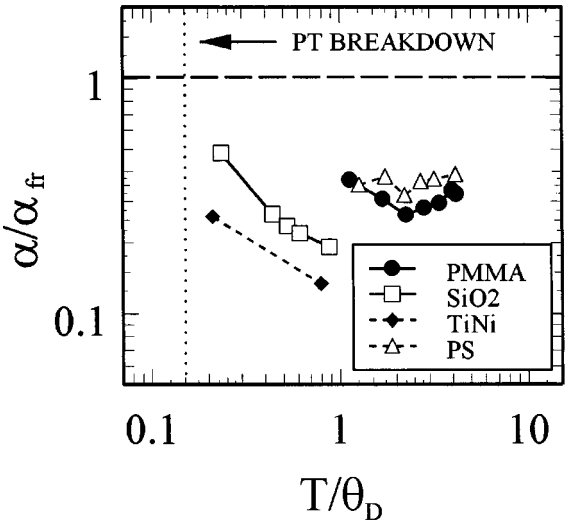

FIG. 12. Ratio of the magnitude of the ω^2 dependence of the attenuation to the prediction of the fracton model [Eq. (7)], $\alpha/\alpha_{\rm fr}$, versus T/Θ_D, for PMMA, PS, a-TiNi, and a-SiO_2. The vertical dashed line at $T/\Theta_D=0.15$ marks the breakdown of perturbation theory in the fracton model.

The fracton predictions for the attenuation are within an order of magnitude of our results over the range $0.2<T/\Theta_D<5$ for all the glasses studied in Fig. 12. The ratios $\alpha/\alpha_{\rm fr}$ fall within the range between 0.1 and 0.5, whereas the experimental results for the attenuation shown in Fig. 5 vary in magnitude by a factor of 40 between PS and TiNi. Considering that the fracton model gives a very simplified description of a real glass, the correlation found between the experiment results and the fracton predictions is surprisingly good.

To achieve a more direct comparison with the predictions of the fracton model it would be desirable to extend our measurements down to lower temperatures such that $T/\Theta_D<0.1$. Unfortunately, this is very difficult to accomplish because of heating of the sample by the laser pulse. Alternatively, if other theories describing the hopping conductivity in glasses are valid for temperatures $T\gg T_0$, it may be instructive to compare our attenuation results with the predictions of such theories. For example, Böttger and Damker[29] have carried out calculations of the hopping con-

ductivity of localized optic modes using a model Hamiltonian system. They obtained results for the hopping conductivity for temperatures as high as $T/\Theta_D \simeq 1$. It would be interesting if these calculations were extended to include the decay rate of phonons caused by hopping of the optic modes in this temperature range.

The variation in sound velocity with frequency and temperature, caused by the hopping process given by Eq. (6), has been calculated by Jagannathan and Orbach.[71] They performed a Kramers-Kronig analysis of Eq. (7) and to lowest order in ω/ω_c obtained a result for the change in sound velocity, relative to the value at $T=0$, which can be written in the form

$$\frac{\delta v(\omega,T)}{v} = -\frac{v\omega_c}{\pi}\frac{\alpha_{\rm fr}(\omega,T)}{\omega^2}[1-(\omega/\omega_c)^2]. \qquad (8)$$

We note that Eq. (8) is just one contribution to the temperature dependence of the sound velocity; the sound velocity is also affected by thermal expansion and other anharmonic effects. These other contributions, however, are independent of frequency. For $\omega \ll \omega_c$ the contribution (8) to the velocity is also frequency independent, whereas for frequencies approaching ω_c a dispersion of the velocity with frequency is predicted which should increase with increasing temperature. If in Eq. (8) we use the experimental values of $\alpha(\omega,T)/\omega^2$ for PMMA, we can calculate the variation with frequency of the temperature dependence of the sound velocity as described by the parameter $\beta = d\ln v_s/dT$. We find that $\beta(130\ \text{GHz}) - \beta(195\ \text{GHz}) = 4\times10^{-5}\ \text{K}^{-1}$ for temperatures from 80 to 300 K. Unfortunately, the difference between these two values of β is just within the experimental uncertainty of our results shown in Fig. 9.

C. Relation to other theories

Buchenau and co-workers[13] have shown that the soft-potential model is capable of explaining many of the attenuation results obtained by Brillouin-scattering and tunnel-junction experiments in an elegant way, but their theory does not appear to predict a quadratic frequency dependence of the attenuation for the frequency and temperature ranges we have measured. More recently, Kozub *et al.*[72] have considered attenuation processes which involve inelastic scattering of phonons from soft modes; however, none of these processes appears capable of explaining our observations for α.

The theory of Allen and Feldman[30] and the numerical simulations of Feldman *et al.*[31] and Sheng and Zhou[32] all suggest that the rise in thermal conductivity above the plateau can be understood in terms of the dynamics of structurally disordered *harmonic* systems. It is assumed that anharmonic processes are unimportant for the description of the thermal conduction at high temperatures; the conduction is assumed to be limited by elastic-scattering processes arising from the disorder. In these studies, tunneling and relaxational attenuation processes for low-frequency phonons are added at a phenomenological level to fit the behavior of $\kappa(T)$ at low temperatures. Within these theories, as currently developed, it would appear that the attenuation in our temperature and frequency range should be independent of temperature. To explain the temperature dependence observed experimentally one would have to consider the anharmonic interaction between the sound wave and the thermal phonons, these phonons having complex displacement patterns due to the disorder in the system. It would be interesting to see whether this incorporation of anharmonicity into the model of Allen and Feldman, or of Sheng and Zhou, would give the right answer for the attenuation.

In the future we plan to examine the transition from crystal to glass by performing attenuation measurements on a series of samples which are implanted with varying doses of ions. It would also be interesting to extend the measurements for polymers to temperatures in the vicinity of the glass transition.

ACKNOWLEDGMENTS

This work was supported by the DOE Grant No. DE-FG02-86ER45267. We thank R. Orbach and J. I. Dijkhuis for valuable discussions, T. Kirst and J. Ding for help in use of the Brown microelectronics facilities, and J. Kyung for AFM surface-roughness measurements on the PMMA samples. We also thank E. Shahoian and V. Martynov of TiNi Alloy Company for preparing the TiNi films, and G. Collins for sending us characterized polymer samples for the roughness studies. We are gratefully indebted to W. Capinski for use of his novel fiber apparatus for long time-delay measurements on the TiNi samples.

*Present address: Rudolph Research, One Rudolph Road, PO Box 1000, Flanders, NJ 07836.

[1] R. C. Zeller and R. O. Pohl, Phys. Rev. B **4**, 2029 (1971).

[2] See, for example, S. Hunklinger and M. von Schickfus, in *Amorphous Solids: Low Temperature Properties*, edited by W. A. Phillips (Springer, Berlin, 1981), p. 81.

[3] For metallic glasses, this behavior for the specific heat and thermal conductivity is found after subtracting the electronic contribution to these quantities.

[4] For the distinctions between the TLS model and the tunneling model, see W. A. Phillips, in *Amorphous Solids: Low Temperature Properties* (Ref. 2), p. 1.

[5] W. A. Phillips, J. Low Temp. Phys. **7**, 351 (1972).

[6] P. W. Anderson, B. I. Halperin, and C. M. Varma, Philos. Mag. **25**, 1 (1972).

[7] Equation (1) could be made more general, for example, by including the possible variation of v on ω, and the dependence of Λ and v on the polarization of phonons.

[8] A. F. Ioffe and A. R. Regel, Prog. Semicond. **1**, 237 (1960).

[9] V. G. Karpov, M. I. Klinger, and F. N. Ignat'ev, Zh. Éksp. Teor. Fiz. **84**, 760 (1983) [Sov. Phys. JETP **57**, 439 (1983)].

[10] Yu. M. Galperin, V. L. Gurevich, and D. A. Parshin, Phys. Rev. B **32**, 6873 (1985); Yu. M. Galperin, V. L. Gurevich, and D. A. Parshin, Zh. Éksp. Teor. Fiz. **92**, 2230 (1987) [Sov. Phys. JETP **65**, 1257 (1987)]; Yu. M. Galperin, V. G. Karpov, and V. I. Kozub, Adv. Phys. **38**, 669 (1989).

[11] M. A. Il'in, V. G. Karpov, and D. A. Parshin, Zh. Éksp. Teor. Fiz. **92**, 291 (1987) [Sov. Phys. JETP **65**, 165 (1987)].

[12] U. Buchenau, Yu. M. Galperin, V. L. Gurevich, and H. R. Schober, Phys. Rev. B **43**, 5039 (1991).

[13] U. Buchenau *et al.*, Phys. Rev. B **46**, 2798 (1992).

[14] G. Karpov and D. A. Parshin, Zh. Éksp. Teor. Fiz. **88**, 2212

(1985) [Sov. Phys. JETP **61**, 1308 (1985)].
[15] L. Gil, M. A. Ramos, A. Bringer, and U. Buchenau, Phys. Rev. Lett. **70**, 182 (1993).
[16] M. S. Love and A. C. Anderson, Phys. Rev. B **42**, 1845 (1990).
[17] T. C. Zhu, H. J. Maris, and J. Tauc, Phys. Rev. B **44**, 4281 (1991).
[18] U. Buchenau *et al.*, Phys. Rev. Lett. **60**, 1318 (1988).
[19] S. Alexander, C. Laermans, R. Orbach, and H. M. Rosenberg, Phys. Rev. B **28**, 4615 (1983).
[20] In the fracton model, glasses are assumed to be fractal in the mass density, or alternatively in the elastic constants or bond connectivity.
[21] See A. Jagannathan, R. Orbach, and O. Entin-Wohlman, Phys. Rev. B **39**, 13 465 (1989), and references therein.
[22] P. F. Tua, S. J. Putterman, and R. Orbach, Phys. Lett. **98A**, 357 (1983).
[23] A. Aharony, S. Alexander, O. Entin-Wohlman, and R. Orbach, Phys. Rev. B **31**, 2565 (1985); Philos. Mag. B **56**, 949 (1987).
[24] S. Alexander, O. Entin-Wohlman, and R. Orbach, Phys. Rev. B **34**, 2726 (1986).
[25] A. Jagannathan, R. Orbach, and O. Entin-Wohlman, Phys. Rev. B **39**, 13 465 (1989).
[26] P. Andreatch, Jr., and H. J. McSkimin, J. Appl. Phys. **47**, 1299 (1976).
[27] A. Alippi *et al.*, Phys. Rev. Lett. **69**, 3318 (1992).
[28] R. Orbach, J. Non-Cryst. Solids **164-166**, 917 (1993).
[29] H. Böttger and Th. Damker, Phys. Rev. B **50**, 12 509 (1994).
[30] P. B. Allen and J. L. Feldman, Phys. Rev. B **48**, 12 581 (1993).
[31] J. L. Feldman, M. D. Kluge, P. B. Allen, and F. Wooten, Phys. Rev. B **48**, 12 589 (1993); P. B. Allen and J. L. Feldman, Phys. Rev. Lett. **62**, 645 (1989).
[32] P. Sheng and M. Zhou, Science **253**, 539 (1991).
[33] A. J. Scholten, A. V. Akimov, and J. I. Dijkhuis, Phys. Rev. B **47**, 13 910 (1993); A. J. Scholten *et al.*, J. Non-Cryst. Solids **164-166**, 923 (1993).
[34] R. Orbach and A. Jagannathan, J. Phys. Chem. **98**, 7411 (1994).
[35] A. R. Long, A. C. Hanna, and A. M. MacLeod, J. Phys. C **19**, 467 (1986).
[36] J. Wolter and R. E. Horstman, Solid State Commun. **37**, 171 (1981).
[37] W. Dietsche and H. Kinder, Phys. Rev. Lett. **43**, 1413 (1979).
[38] J. Mebert and W. Eisenmenger, Z. Phys. B **95**, 231 (1994).
[39] R. Vacher and J. Pelous, Phys. Rev. B **14**, 823 (1976).
[40] Mira Ti:sapphire laser pumped by either Innova Model 310 or 415 Ar^+ laser from Coherent Inc., Santa Clara, California, 95054.
[41] Poly(methyl methacrylate), molecular weight 496 K from Shipley Company, Inc., Newton, Massachusetts 02162. Measurements on molecular weight 950 K samples gave identical attenuation results.
[42] Poly(styrene) standard, molecular weight 400 K from Aldrich Chemical Co., Milwaukee, Wisconsin, 53201.
[43] Poly(ethyl methacrylate) secondary standard, molecular weight 340 K from Aldrich Chemical Co., Milwaukee, Wisconsin, 53201.
[44] K. R. Collen, A. B. Ellis, J. D. Busch, and A. D. Johnson, in *Phase Transformation Kinetics in Thin Films*, edited by M. Chen *et al.*, MRS Symposia No. **230** (Materials Research Society, Pittsburg, 1991), p. 97.
[45] The *a*-TiNi films were sputtered by TiNi Alloy Company, San Leandro, California, 94577.
[46] For example, see H. G. Tompkins, *A User's Guide to Ellipsometry* (Academic, Boston, 1993).
[47] C. Thomsen, H. T. Grahn, H. J. Maris, and J. Tauc, Phys. Rev. B **34**, 4129 (1986).
[48] R. A. Haldon and R. Simha, J. Appl. Phys. **39**, 1890 (1968).
[49] E. Kato, J. Chem. Phys. **73**, 1020 (1980).
[50] R. Nava, D. Pereira, and L. Amorer, J. Appl. Phys. **69**, 99 (1991).
[51] Y. Wada and K. Yamamoto, J. Phys. Soc. Jpn. **11**, 887 (1956).
[52] Al_2O_3 substrates were ''superfinish'' polished by Meller Optics Inc., Providence, Rhode Island, 02904.
[53] Professor Olaf Weis (Ulm University, Germany) kindly measured the surface roughness of these substrates using stylus profilometry.
[54] T. Abe, E. F. Steigmeier, W. Hagleitner, and A. J. Pidduck, Jpn. J. Appl. Phys. **31**, 721 (1992).
[55] G. W. Collins *et al.*, Phys. Rev. Lett. **73**, 708 (1994).
[56] G. P. Scherg, R. Gartner, P. Berberich, and H. Kinder, *Phonon Scattering in Condensed Matter VII* (Springer, Berlin, 1993), p. 266; G. P. Scherg, Ph.D. thesis, Technical University, Munich, Germany, 1989.
[57] M. Schmidt, R. Vacher, J. Pelous, and S. Hunklinger, J. Phys. (Paris) Colloq. **43**, C9-501 (1982).
[58] D. A. Jackson, H. T. A. Pentecost, and J. G. Powles, Mol. Phys. **23**, 425 (1972).
[59] J. E. Graebner, B. Golding, and L. C. Allen, Phys. Rev. B **34**, 5696 (1986).
[60] PMMA: D. A. Jackson, H. T. A. Pentecost, and J. G. Powles, Mol. Phys. **23**, 425 (1972); PS: R. Vacher and J. Pelous, J. Phys. (Paris) Colloq. **42**, C6-125 (1981); PEMA: Y.-Y. Huang, Ph.D. thesis, Stevens Institute of Technology, Hoboken, 1971; *a*-SiO_2: R. Vacher and J. Pelous, Phys. Rev. B **14**, 823 (1976).
[61] For example, see K. S. Gilroy and W. A. Phillips, Philos. Mag. B **32**, 202 (1980), and references therein.
[62] R. Vacher, J. Pelous, F. Plicque, and A. Zarembowitch, J. Non-Cryst. Solids **45**, 397 (1981).
[63] J. P. Bonnet, J. Non-Cryst. Solids **127**, 227 (1991).
[64] H. J. Maris, *Physical Acoustics, Vol. VIII* (Academic, New York, 1971), p. 279.
[65] H. H. Barrett, Phys. Rev. **178**, 743 (1969).
[66] R. Nava, J. Non-Cryst. Solids **76**, 413 (1985).
[67] J. J. Freeman and A. C. Anderson, Phys. Rev. B **34**, 5684 (1986).
[68] D. G. Cahill and R. O. Pohl, Phys. Rev. B **35**, 4067 (1987).
[69] J. J. Freeman, Ph.D. thesis, University of Leeds, United Kingdom, 1985.
[70] J. R. Matey and A. C. Anderson, Phys. Rev. B **16**, 3406 (1977).
[71] A. Jagannathan and R. Orbach, Phys. Rev. B **41**, 3153 (1990).
[72] V. I. Kozub, A. M. Rudin, and H. R. Schober, Phys. Rev. B **50**, 6032 (1994).